BUILDING ZONE FAULT DETECTION WITH KALMAN FILTER BASED METHODS

Zixiao Shi, William O'Brien, H. Burak Gunay

Department of Civil and Environmental Engineering
Carleton university
Ottawa Ontario, Canada

ABSTRACT

Fault detection and diagnostics (FDD) is important to maintain proper operation of the building systems. However, most research is focused on heating, ventilation and air conditioning (HVAC) systems FDD, while little work has been done on zone level diagnostics. A building zone is a complex system, but usually equipped with fewer sensors, making the FDD process very challenging. A Bayesian Filter can be used to recursively learn states and parameters of a dynamic system with a limited number of measurements, making it a potential candidate for thermal zone FDD applications. The study in this paper implements a fault detection algorithm for thermal zones using Kalman Filter-based methods with a reduced order energy balance model, and tests its performance using both simulation and experimental data.

INTRODUCTION

Building operation is often sub-optimized, and by maintaining properly, buildings' energy consumption can be reduced by 20% to 30% [Roth et al., 2005]. Fault detection and diagnostic (FDD) can be used to detect and diagnostic operation faults caused by improper installation, maintenance or equipment failure. Most fault detection and diagnostics research has been focused on HVAC systems and whole building performance [Katipamula and Brambley, 2005b]. The potential of implementing a distributed FDD system in each individual zone could be complimentary to the current research. However, unlike HVAC systems, building zones are mostly non-stationary, their normal operation could be altered by change of use and occupant behaviour very easily. This brings unique challenges to the building zone FDD applications.

LITERATURE REVIEW

An ideal fault detection and diagnostic system should have those following characteristics [De Kleer and Williams, 1987]: low cost, reliable and low false positive rates. Katipamula and Brambley have provided an excellent two-part review of FDD and prognostics in building systems [Katipamula and Brambley, 2005b, Katipamula and Brambley, 2005a] and classified building systems FDD methods into two groups: model based methods and data driven methods.

Rule based or "expert" systems, part of the model based methods, are well developed and are often heuristic based [Katipamula and Brambley, 2005a]. An example of the "expert" system is the APAR system developed by Schein et al. [Schein et al., 2006]. Rules implemented in those systems are usually predefined and require manual updates [Katipamula and Brambley, 2005a]. While rule based methods are suitable for air handling unit (AHU) FDD since mechanical systems are usually stable and well monitored, it may become costly to implement in zone level FDD due to the manual workload required to design and update predefined rules for each different zone characteristics. Some rule based diagnostic systems can be dynamically updated such as the one proposed by Rossi et al. for vapor compression cycles [Rossi and Braun, 1997], but they often use optimization and require a large set of historical data to train and update the rules and this process requires a large

Table 1: FDD Methods Comparison

	FDD Cost	Parameter Estimation	Update Method	Update Cost
"Expert" Method	Low	No	Manual/Process history data	High
Quantitative Model Based	High	Only during updates, overfit issues	Manual/Process history data	High
Black-box Method	Low-High	No	Process history data	Medium-High
Grey-box Model Based	Low-Medium	Only during updates	Process history data	Medium-High
Regular Filters	Low	No	Recursive	Low
Kalman Filters with Grey-box Model	Low-Medium	Recursive	Recursive	Low

computation power.

Another type of model based method, FDD systems using quantitative models are built on physics or engineering principles. Those systems are capable of simulating fault stage and providing precise FDD results, but they are often too complex to implement and require too many sensors to function properly [Venkatasubramanian et al., 2003]. Those systems can also be calibrated using a large set of process history data and optimization functions, but quantitative zone models with high-dimensional inputs are prone to over-fitting problems due to limited number of sensors typically installed in a building zone. A overfitted model cannot provide accurate predictions and loses meaningful information about the physical properties of the zone.

Data driven methods, or process history methods, consist of black-box methods and grey-box model based methods that mainly use operation data to train their models. Black-box methods are purely based on statistical learning algorithms. A lot of research has been done on developing black-box methods such as a chiller systems FDD method using principal component analysis proposed by Wang et al. [Wang and Cui, 2005], and a building level energy consumption FDD method using various data mining techniques used by Capozzoli et al. [Capozzoli et al., 2015]. Black-box models may provide a better fit to the zone operation data, making abnormal operation easier to identify. However, they do not provide any information about the physical properties of the system they represent, thus making it difficult to pinpoint the fault cause.

Grey-box models are simplified physical models - they are not as accurate as white-box models but are much faster to compute. Lower number of parameters used in those models often make them less prone to over-fitting issues. Grey-box models such as the one proposed by Braun et al. [Braun and Chaturvedi, 2002] have been used in many building control applications [Henze et al., 2004, Braun, 2003, Ma et al., 2012, Gunay et al., 2014]. Still many grey-box methods use optimization to train their parameters, thus requiring a large set of historical data and significant processing power during each update. This makes them costly to implement on zone controllers due to limited memory and computation power. A recursive or filter based grey-box FDD method requires much less computation power, as it updates existing parameters during each iteration. Gunay et al. proposed a method using extended Kalman filter (EKF) and a first order thermal model for zone predictive control, and demonstrated accurate predictions as well as large potential energy savings [Gunay et al., 2014]. Usoro et al. used an extended Kalman filter to perform HVAC FDD tasks and showed promising results[Usoro et al., 1985]. Mulumba et al. have also demonstrated application of Kalman filter based methods for air handling unit FDD applications, the resulted fault detection rate is reasonable but sometimes is quite slow to pick up the fault due to the recursive learning process [Mulumba and Friedrich, 2014]. However, usage of Kalman filter based methods to estimate parameters in FDD process has rarely been discussed.

Table 1 shows a comparison between the different FDD employed in building applications. For building zone FDD applications, parameter estimation is important for fault isolation due to limited sensing capability,

and updates are often required to reflect change of occupant behaviours and zone characteristics. Due to those requirements Kalman filters with grey-box models could be a good candidate for zone level FDD.

SCOPE

The scope of this paper is to propose a multi-agent based FDD method using extended Kalman filter and demonstrate its functionalities as a proof of concept. An experiment was also conducted to generate normal operation data and data during faulty operations with both experimental data and simulation results, but only a limited number of fault cases were used. A more comprehensive test and comparison study with other existing FDD methods are part of the future work.

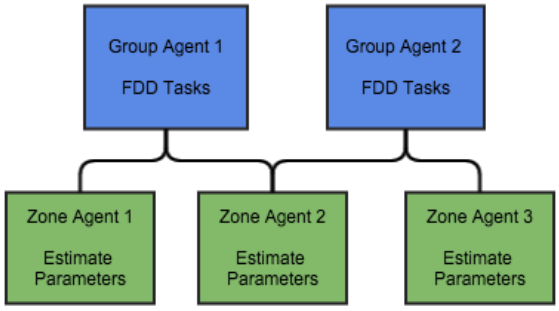

Figure 1: System Architecture

METHODOLOGY

SYSTEM ARCHITECTURE

The multi-agent FDD system in this paper contains two types of agents: zone agents and group agents. Group agents use estimated physical parameters and state predictions sent from their zone agents to perform FDD tasks and update its FDD parameters. The agents are designed to run on a distributed system – zone agents run independently on local controllers, while group agents are installed on more powerful central controllers or building energy management system servers. The relation between the zone agents and the group agents is many-to-many, which means one zone could belong to multiple groups. This structure enables different FDD archetypes from multiple group agents could be adopted for a same zone if required. The relations of the agents are currently static and predefined. Self-organizing agents may be possible to implement in the future so that a zone could migrate to different group(s) automatically should the zone change its characteristics during the operation.

Diagnosing zones in groups means more information is available from multiple similar zones than from a single zone. Since occupant behaviour has a significant impact on a zone's thermal response, aggregating multiple zones to produce a normal operation range could potentially normalize the effect of occupant behaviour. Users can still create one group agent for each of the zones to establish FDD agent for each single zone if needed.

This distributed architecture also allows asynchronous processing, making the whole network more robust as missing or off-line agents won't affect the whole FDD process. It also allows zone agents to be implemented on existing local controllers without extra need of equipments, thus reducing the overall cost.

ZONE AGENT

The zone agent is built on an extended Kalman filter with grey-box models to perform state prediction and parameter estimation. A filter is often used to predict future states for dynamic systems recursively and involves two steps: the predict step and the update step. The predict step uses past knowledge and control inputs to predict the future states, then during the update step residual is calculated by the difference of the prediction and the measurement of states and used to correct the filter parameters. The Kalman filter is one of the most widely used filters, and the extended Kalman filter (EKF) is an approximation of nonlinear systems developed from the basic Kalman filter. Extended Kalman filters often use simplified physical models as its prediction model, so parameters conveying physical meanings of the system can also be estimated using a joint estimation technique assuming the parameters are virtual states. However, the extended Kalman filter is not an optimal estimator and is very sensitive to initial conditions which makes them diverge very quickly if the initial condition is not set properly. So the initial condition for the EKF needs to be cautiously set.

For the predict step of the EKF, state vector and covariance matrix are estimated using the current control input:

$$\hat{x}_{k|k-1} = f(\hat{x}_{k-1|k-1}, u_{k-1}) \tag{1}$$

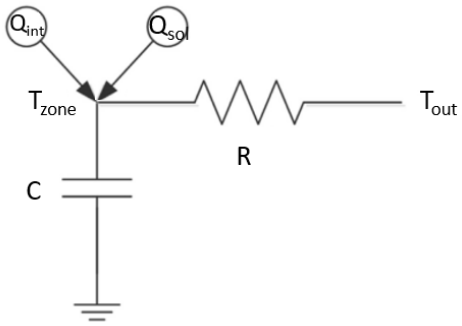

Figure 2: Thermal Model

$$P_{k|k-1} = F_k P_{k-1|k-1} F_k^T + Q_k \tag{2}$$

Where x is the state vector, u is the control vector and $\hat{x}$ is the predicted state estimate. f is the state function that transforms state estimate and control vector at the timestep $k-1$ to predict the future state at the next timestep k. f is also the grey-box model which will be established in the later section. Q and R are the covariance matrices for the process noise and the observation noise, typically with a zero mean Gaussian distribution. P is the predicted covariance matrix. The state transition matrix F used for the covariance estimation is derived by taking the Jacobian of the state function f:

$$F_{k-1} = \frac{df}{dx}\Big|_{\hat{x}_{k-1|k-1}, u_k} \tag{3}$$

And for the update step, the difference(residual) between the measured and predicted state vector is used to update the filter:

$$\widetilde{y_k} = z_k - h(x_{k|k-1}) \tag{4}$$

$$S_k = H_k P_{k|k-1} H_k^T + R_k \tag{5}$$

$$K_k = P_{k|k-1} H_K^T S_K^{-1} \tag{6}$$

$$P_{k|k} = (I - K_k H_k) P_{k|k-1} \tag{7}$$

$$\hat{x}_{k|k} = \hat{x}_{k|k-1} + K_k \widetilde{y_k} \tag{8}$$

Where $\widetilde{y}$ is the measurement residual, z is the measurement, S is the residual covariance, K is the Kalman gain. h is the measurement function which determines the state parameters used for residual calculation from the state vector. The observation matrix, H, is obtained by taking the Jacobian of the measurement function h:

$$H_k = \frac{dh}{dx}\Big|_{\hat{x}_{k-1|k-1}} \tag{9}$$

A first order energy balance model is used to predict the indoor air temperature state, as shown in Figure 2. Gunay et al. demonstrated that a simple R-C model is capable of predicting the performance of a thermal zone accurately, whereas higher order models may have over-fitting problems and sensitive to improper initial condition[Gunay et al., 2014]. Thus a simple thermal model was selected for the EKF. The model function based on available sensors is:

$$\begin{aligned} dT = {} & T(\frac{-dt}{RC}) + T_{out}(\frac{dt}{RC}) + E_{lux}(\frac{\rho_{lux} dt}{C}) \\ & + Occu(\frac{Q_{int} dt}{C}) + Rads(\frac{Q_{rad} dt}{C}) \\ & + \sqrt{p_{vav}}(T_{sat} - T)(\frac{\rho_{air} dt}{C}) + \frac{Q_{cons}}{C} \end{aligned} \tag{10}$$

The model estimates indoor air temperature change using available sensors installed in the experiment setup. T is the indoor air temperature, T_{out} is the outdoor air temperature, E_{lux} is the luminance measured from the ceiling, $Occu$ is the occupancy state, $Rads$ is the on/off state of the radiant panel, p_{vav} is the dynamic pressure of the supply air and T_{dat} is the supply air temperature.

For the physical parameters, R is the overall thermal resistance between the zone air and outdoor air, C is the overall thermal capacitance of the zone, ρ_{lux} is the ratio between the combined electrical lighting and solar thermal radiation into the zone and measured luminance level, Q_{int} is the extra thermal load caused by occupant and equipment use, Q_{rad} is the thermal energy received from the radiant panel when on, ρ_{air} is the supply air specific heat of the combined the supply air temperature difference and flow (square root of supply pressure), and Q_{cons} is the constant heat gain caused by standby power consumption (phantom load).

State function f is then derived from the model function using timestep ΔT:

$$T_k = T_{k-1} + dT_{k-1} \Delta t_{k-1} \tag{11}$$

And for the update of parameter estimation x_p, they become:

$$x_{p,k} = x_{p,k-1} \tag{12}$$

After the model is formalized, control vector u is comprised of sensor inputs, while model parameters and the indoor air temperature form the state vector x:

$$u = \begin{bmatrix} u_1 \\ u_2 \\ u_3 \\ u_4 \\ u_5 \end{bmatrix} = \begin{bmatrix} T_{out} \\ E_{lux} \\ Occu \\ Rads \\ \sqrt{p_{vav}}(T_{sat} - T) \end{bmatrix}$$

$$x = \begin{bmatrix} x_1 \\ x_2 \\ x_3 \\ x_4 \\ x_5 \\ x_6 \\ x_7 \end{bmatrix} = \begin{bmatrix} T \\ \frac{dt}{RC}\Delta t \\ \frac{\rho_{lux} dt}{C}\Delta t \\ \frac{Q_{int} dt}{C}\Delta t \\ \frac{Q_{rad} dt}{C}\Delta t \\ \frac{\rho_{air} dt}{C}\Delta t \\ \frac{Q_{cons}}{C}\Delta t \end{bmatrix}$$

The overall state function for the EKF is then:

$$f(x,u) = \begin{bmatrix} x_1 - x_1x_2 + u_1x_2 + u_2x_3 + \\ u_3x_4 + u_4x_5 + u_5x_6 + x_7 \\ x_2 \\ ... \\ x_7 \end{bmatrix}$$

Since in the state vector only indoor air temperature T is measured by a sensor, the measurement matrix is then:

$$h(x) = \begin{bmatrix} x_1 \\ 0 \\ ... \\ 0 \end{bmatrix}$$

Residual in this case is directly the difference between the measured and the predicted indoor air temperature.

In this zone agent, the effects of occupancy and equipment usage are approximated by the occupancy sensor; where as incident radiation and electrical lighting gain are aggregated by the luminance sensor. If more sensors are available such as electricity sub meter and direct measurement of solar radiation through the window, the model could be expanded and more information will be available for fault detection and diagnostics.

GROUP AGENT

Unlike many FDD methods which use residual to detect faults, in this FDD method the group agents perform FDD tasks by detecting if each estimated zone parameters are within its group's normal operation range. Even though residual may be useful to detect abnormal operation, it does not provide any additional information to diagnose and narrow down the potential fault cause(s). On the contrary physical parameters estimated by the zone agents provide more insight into the zone behaviour. Residual analysis is still investigated but is not the focus of this paper. The overall FDD task performed in the group agent is shown in Figure 3.

The normal operation range for each estimated parameter is obtained from the average and the standard deviation of all related zone parameter estimates. A parameter tolerance setting determines the width of the normal operation range. Lower tolerance causes higher FDD sensitivity which leads to higher false-positive rate and lower false-negative rate, and vice versa. The parameter tolerance could be tweaked during operation, and possibly adjusted dynamically to achieve optimal FDD performance. In this paper a constant high parameter tolerance is used, and the normal operation range is bounded by average estimated parameters plus/minus *three* standard deviations. The normal operation range is also updated by new zone parameter estimates, if the zone status is normal. If the normal operation range is remain constant, operation state of the zone agent could also be changed to "No Updates".

In order to find the cause of abnormal parameters and isolate the potential faults, cause-effect relations between the fault causes and abnormal parameters estimated by each zone agent are needed. The cause-effect relations used in the proposed method is shown in Figure 4. Once an abnormal estimated parameter is detected by the group agent, the potential fault causes are traced by the cause-effect relations. In this paper the fault diagnostics process is performed manually to confirm the fault detection capability of the proposed system.

Once fault(s) are found, they are stored in a fault list and awaits manual or automatic confirmation. The related estimated parameter(s) are also stored in the fault list and not used for normal range update until a confirmation is received. If a fault is confirmed, then the operation state of the zone is changed to "Faulty" and it's parameter estimates are no longer used for normal operation range updates inside zone agents. In this paper all faults are automatically confirmed.

AGENTS INITIALIZATION

Before the FDD system is ready, an initialization period is needed in order to stabilize the state vectors inside

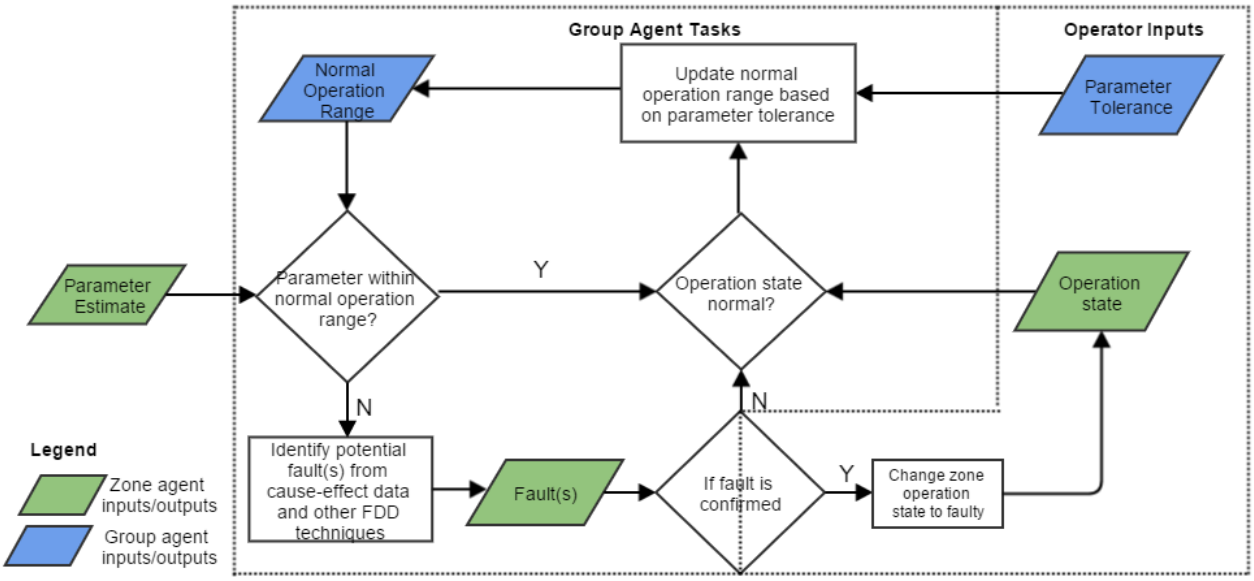

Figure 3: FDD Task Flowchart

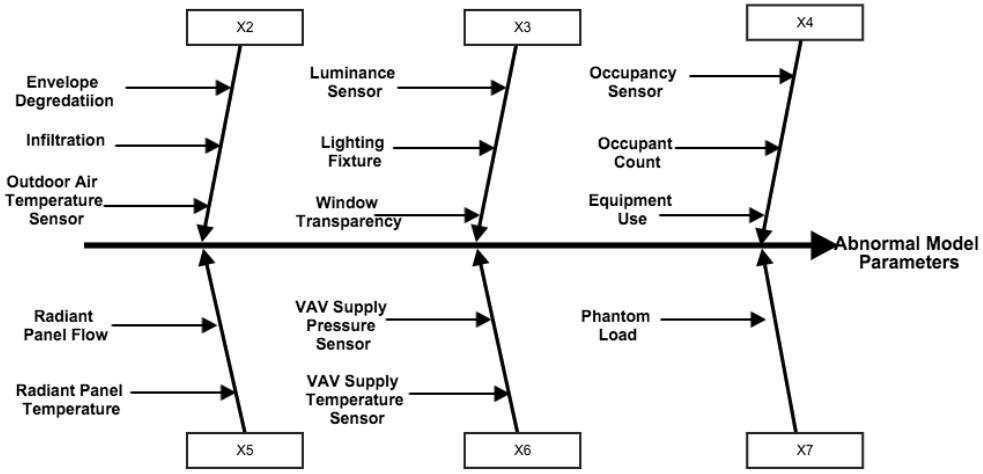

Figure 4: Cause-Effect Diagram of the Proposed FDD Method

zone agents. Since inappropriate initial condition can lead to divergence in EKF, multiple zone agents for each zone with different initial conditions are needed to be trained simultaneously during this period. After the initialization period, only agents with valid parameter estimations are kept. For this FDD method, the estimated parameters should be higher than zero and lower than certain values depending on the prediction timestep. In the future proper initial condition can also be predetermined using building simulation results and optimization to reduce the length of this initialization process.

For new buildings the agents can be initialized during the commissioning period during which all systems are ensured to be running under the design condition. And for applications in existing buildings, the related buildings systems have to be audited first to ensure their measurer performance represents normal operation conditions.

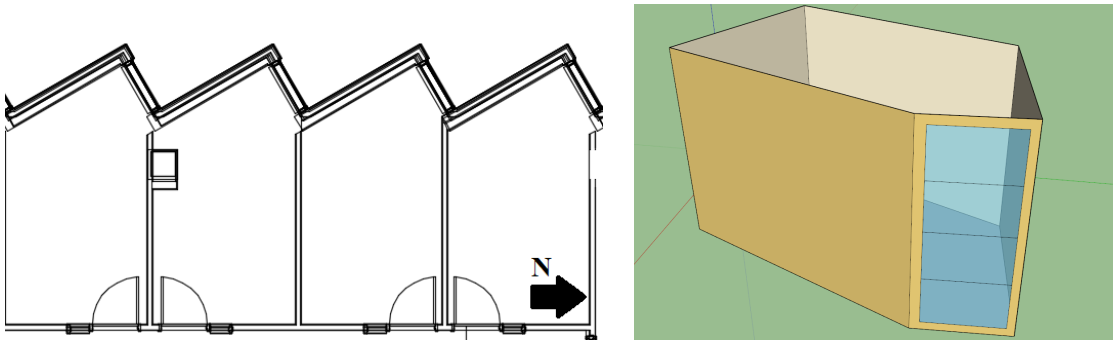

Floor Plan EnergyPlus Model

Figure 5: Zone Information

EXPERIMENT SETUP

An experiment was carried out to test the applicability of the proposed FDD method. Sensor data from five neighbouring private offices with identical floor plans were gathered in Carleton University. Data used in this paper were measured during the summer cooling months from May till end of June, so the radiant panels were always off and parameter x_5 ignored. All systems inside those offices were assumed to be operating under design conditions. An EnergyPlus model was calibrated to represent the average performance of those office zones. The internal walls are assumed to be adiabatic, the external walls have an insulation level of 2.75RSI and the windows have a u factor of $2.05 W/m^2K$. The occupancy of the energy model is from 9:00am to 17:00pm with one occupant in each office. Infiltration rate is 0.5 air change per hour. The floor plan and energy model are shown in Figure 5.

Six zone agents and one group agent were initialized using the collected data. A time step of 15 minutes was used. Since the data were collected previously, all agents performed their tasks synchronously. The whole data period was used for agent initialization and best initialization length was discovered.

Additional datasets were created to emulate possible faults in those offices. Sensor faults such as blocked VAV box pressure sensor, blocked luminance sensor and thermostat temperature sensor bias were created by altering the measurement data from one of the five offices. Other faults such as insulation degradation and increased air leakage were created through simulation by altering the calibrated EnergyPlus model. It is noteworthy that due to the limitation of EnergyPlus, many faults, such as sensor faults, could not be simulated without extensive use of its Energy Management System. There is also a lack of literatures about using energy simulation as a way of recreating possible zone faults. Creating fault cases using energy simulation needs further research.

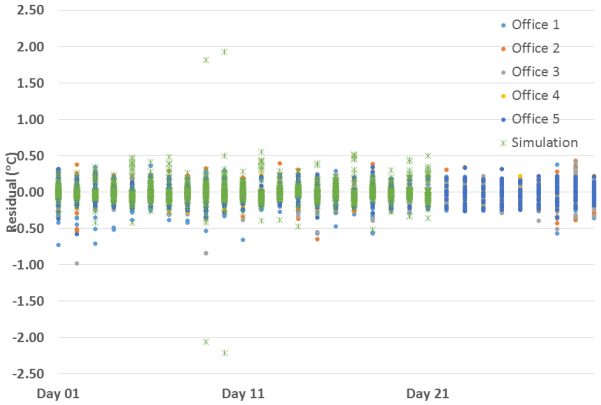

Figure 6: Experiment Prediction Residual

RESULTS AND DISCUSSION

NORMAL OPERATION RESULTS

Before analyzing the performance of the zone agents, an initialization period of seven days was used to stabilize the estimated parameters. All data analyzed later in this section are after the initialization period.

To determine if the proposed zone agent could represent its zone performance adequately, firstly the prediction residual needs to be low. Figure 6 displays the resid-

Table 2: Estimated Parameters After Agent Initialization

	x2 ($\times 10^{-3}$)	x3 ($\times 10^{-4}$)	x4 ($\times 10^{-2}$)	x6 ($\times 10^{-3}$)	x7 ($\times 10^{-2}$)
Office 1	4.73	4.46	0.97	3.38	4.04
Office 2	4.24	3.67	1.55	3.54	1.86
Office 3	4.63	3.71	Unoccupied	3.19	1.50
Office 4	4.75	3.64	1.99	3.67	2.58
Office 5	4.87	3.72	2.01	3.76	2.66
EP Model	4.81	3.23	1.00	Not Applicable	2.01
Normal Operation Range	4.00–5.35	2.54–4.93	0–2.99	2.83–4.19	0–5.38

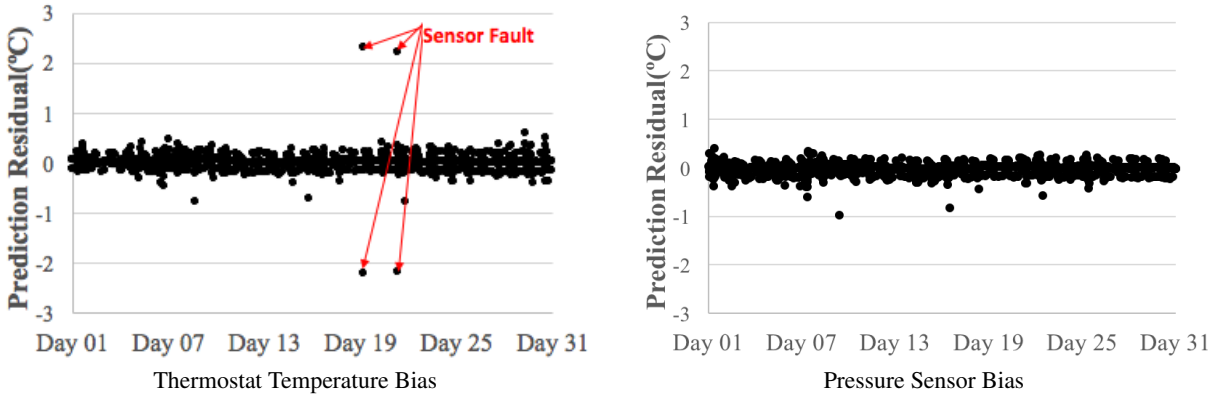

Figure 7: Residuals of Predicted State and Input State Measurement Biases

uals of the measured and simulated data. In most cases the residuals from the measured data are within $\pm 0.5^oC$, and never exceeds the $\pm 1.0^oC$ range. However, for the EnergyPlus Simulation data, in several occurrences the prediction residual is outside the $\pm 1.0^oC$ range and is probably caused by the way EnergyPlus calculates energy balance and mechanical system response.

Table 2 shows the average state variables obtained. The estimated state parameters have very small variations, confirming the assumption that similar rooms would produce similar grey-box model responses. Since office 3 was unoccupied, its parameter related to occupancy was ignored. And for the EnergyPlus model, supply pressure was not available from the output list, supply flow rate was used instead. Due to this reason, parameter x_6 was also omitted from the comparison. Note that parameter x_4 and x_7 have higher variations than others due to the differences of equipment loads and occupant's usage in each of the office, while the unoccupied office 3 has the lowest phantom load parameter (x_7). Also wall constructions and window properties of the zones should be the most consistent parameters than other characteristics, and the parameter x_2 agrees with this assumption, since it has the lowest variation among other estimated parameters.

Overall the results obtained using normal operation data are consistent with assumptions, and proves that the proposed zone agent could well represent different zone characteristics with the estimated parameters convey meaningful physical information. However, how to better use energy simulation results as training data still requires further investigation.

FDD USING RESIDUAL

Before conducting FDD tests with proposed group agent, the ability of performing FDD using residual is investigated. Since the proposed FDD method learns from the thermal zone data recursively, any sudden changes

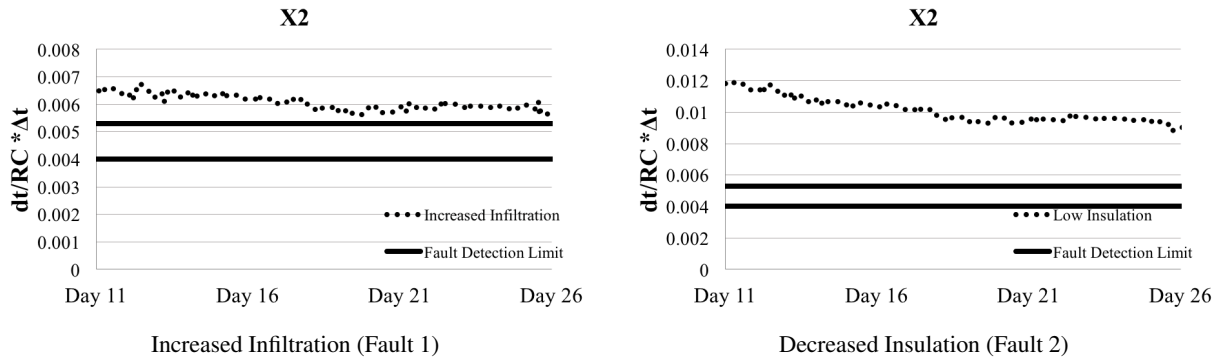

Increased Infiltration (Fault 1) Decreased Insulation (Fault 2)

Figure 8: Zone Envelope Degradation with Increased X_2 Values

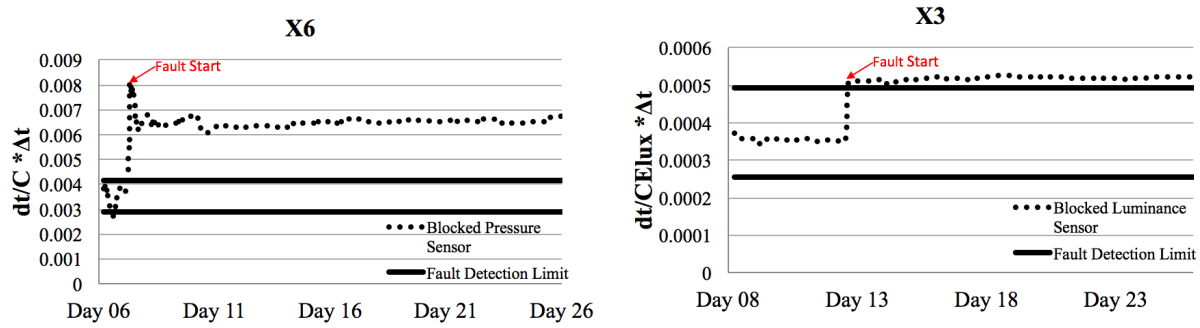

Blocked VAV Box Pressure Sensor (Fault 3) Blocked Luminance Sensor (Fault 4)

Figure 9: Blocked Sensors with High Parameter Estimates

from the measured thermal response caused by sensors or system failures could be easily identified by large measurement residuals. Figure 7 shows higher residual values occurs when a 20% temperature sensor bias is introduced to the data (left); on the other hand, while a large measurement error of 300% is introduced to the pressure sensor in the VAV box, the resulted residual is much lower. Only the direct measurement of the predicted state can have a large impact on residual. Measurement residual alone cannot isolate or diagnostic the origin of the fault, nor it is sensitive to all possible faults. This further confirms that while measurement residual may be useful when monitoring sudden changes of the temperature measurement, physical parameters from the grey-box model may provide better fault diagnostics and isolation capabilities.

GROUP AGENT FDD

This section demonstrates the ability of the proposed group agent FDD process as a proof of concept. The normal operation range is obtained using the normal operation data. Average state parameters learned from the fault cases are presented in Table 3. A seven day warm up period was used in in order to stabilize the parameters. Parameter values outside the normal operation range (three standard deviations from average) are highlighted in the table.

For the first two fault cases, suboptimal operations caused by envelope degradations were investigated. The fault cases were simulated by modifying the calibrated EnergyPlus model. The values of the affected parameters (x_2) are shown in Figure 8. In the first case the infiltration rate was increased to 0.8ACH from 0.5ACH, and in the second case the overall envelope insulation level was halved. While all other state parameters remained close to the typical operational values, x_2 val-

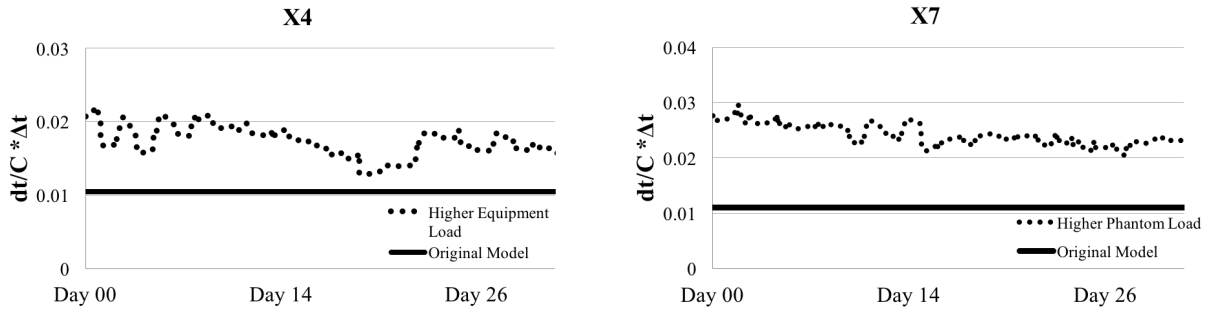

High Equipment Load

High Phantom Load

Figure 10: Suboptimal Operation Due to High Internal Loads

	Increased Infiltration	Decreased Insulation	Pressure Sensor Fault	Luminance Sensor Fault	Higher Equipment Load	Higher Phantom Load
x2	$\mathbf{6.01 * 10^{-3}}$	$\mathbf{8.92 * 10^{-3}}$	$4.93 * 10^{-3}$	$4.93 * 10^{-3}$	$4.62 * 10^{-3}$	$4.63 * 10^{-3}$
x3	$3.18 * 10^{-4}$	$3.11 * 10^{-4}$	$3.16 * 10^{-4}$	$\mathbf{5.11 * 10^{-4}}$	$3.23 * 10^{-4}$	$3.20 * 10^{-4}$
x4	$1.01 * 10^{-2}$	$1.10 * 10^{-2}$	$2.07 * 10^{-2}$	$1.99 * 10^{-2}$	$1.65 * 10^{-2}$	$1.10 * 10^{-2}$
x6	Not Applicable	Not Applicable	$\mathbf{6.56 * 10^{-3}}$	$3.14 * 10^{-3}$	Not Applicable	Not Applicable
x7	$1.82 * 10^{-2}$	$1.65 * 10^{-2}$	$3.01 * 10^{-2}$	$2.42 * 10^{-2}$	$1.36 * 10^{-2}$	$2.46 * 10^{-2}$

Table 3: Faulty Operation Model Parameters (bold text represents abnormal parameter)

ues in both cases were increased significantly. The increased x_2 value means the thermal response is more sensitive to the outdoor temperature, and from the cause-effect relation data it can be concluded that three possible faults might have caused this problem: envelope degradation, infiltration and outdoor air temperature sensor bias. However, if the outdoor air temperature sensor is faulty, all other zones that use its data will also have abnormal x_2 parameter since its reading is shared by all zones. By combining the proposed FDD method and simple logic it can be deduced that the fault is caused by envelope degradation and/or increased infiltration.

Two other cases with faulty sensors were then recreated. Figure 9 shows the impact of those sensor faults and their affected state parameters. For the VAV box pressure sensor fault, the sensor was assumed to be blocked and produced 10% of the actual reading. And for the luminance sensor, the fault was assumed to be also measuring 10% of the actual reading. In both cases the related parameters exhibit large changes caused by sensor faults and lead to higher values than typical operations. Higher x_3 and x_6 values indicate the measurements may be lower than the actual values, thus the changes in the parameters confirms the two faulty sensor cases.

The impacts of increased equipment load and occupant usage were also investigated using energy simulation. For occupant equipment load and phantom load the normal operation range is very wide due to the variations of each office's use, so only deviations from original operation were analyzed. Figure 10 shows the suboptimal operation caused by very high equipment load and phantom load compared to the calibrated model. For the high equipment load, the zone electrical equipment load was assumed to be doubled of the calibrated model. Parameter x_4 related to occupancy and equipment load has seen a 50% increase than that of the calibrated model, but still within the typical usage range. In the increased phantom load case, electricity usage schedule during the unoccupied period was changed to 50% instead of 10%, and the constant heat gain parameter x_7 was increased by more than 100% compared to the original energy simulation.

Most of the fault cases used here have significant im-

pact on the zone response. In the future a more comprehensive list of faults will be tested to further analyse the capabilities of the proposed FDD method. More importantly faults related to a single parameter might affect other parameters due to the way extended Kalman filter performs update. So it is possible concurrent multiple faults might keep the state parameters within the normal operation range, thus unable to be detected.

DISCUSSIONS AND FUTURE WORK

This paper has demonstrated the potential of using a grey-box model based extended Kalman filter for zone level fault detection and diagnostics. While the prediction residual is capable of identifying sudden changes in the thermal zone responses, model state parameters could be used to further perform this task. However at this early stage there are a lot of future research required:

1. The initial condition is critical to the extended Kalman Filter, and the state parameters could diverge quickly if the initial values are set incorrectly or very noisy data has been encountered. This limits the applicability of the method. Many techniques that can be applied to offset this issue such as parameter initialization with least-square curve fitting and constrained extended Kalman Filter are under investigation.

2. Currently similar zones are determined by human input. By using building information model and some statistical methods such as clustering, grouping of similar zones could be performed automatically and dynamically throughout the operation.

3. In this paper the sensor faults were introduced artificially to the measured data, so the control system response has been ignored. In the future real experiments such as modified sensor calibrations could include the response of the zone controls.

4. Zone mass balances such as CO_2 concentration and air moisture mass balances could also be implemented into the extended Kalman filter. This provides redundancy of sensor measurement usage and provides more information about the zone performance. For example, if the infiltration rate is increased, both the energy balance model and CO_2 mass balance model will be affected.

5. Integration with other fault detection techniques and establish an integrated fault diagnostics system.

CONCLUSION

This paper proposed a multi agent fault detection method for building zones using extended Kalman filter. A linear grey-box model was used in the extended Kalman filter to obtain physical information about zone performance. Overall the method proposed in this paper has been able to detect most of the fault cases created, but multiple faults may cause the method to perform poorly. Also, only limited cases of faults were created for this paper, further tests with more faults can further validate the performance of this method.

REFERENCES

[Braun, 2003] Braun, J. E. (2003). Load control using building thermal mass. *Journal of solar energy engineering*, 125(3):292–301.

[Braun and Chaturvedi, 2002] Braun, J. E. and Chaturvedi, N. (2002). An inverse gray-box model for transient building load prediction. *HVAC&R Research*, 8(1):73–99.

[Capozzoli et al., 2015] Capozzoli, A., Lauro, F., and Khan, I. (2015). Fault detection analysis using data mining techniques for a cluster of smart office buildings. *Expert Systems with Applications*, 42(9):4324–4338.

[De Kleer and Williams, 1987] De Kleer, J. and Williams, B. C. (1987). Diagnosing multiple faults. *Artificial Intelligence*, 32(1987):97–130.

[Gunay et al., 2014] Gunay, H. B., Bursill, J., Huchuk, B., Brien, W. O., and Beausoleil-morrison, I. (2014). Shortest-prediction-horizon model-based predictive control for individual offices. *Building and Environment*, 82:408–419.

[Henze et al., 2004] Henze, G. P., Felsmann, C., and Knabe, G. (2004). Evaluation of optimal control for active and passive building thermal storage. *International Journal of Thermal Sciences*, 43(2):173–183.

[Katipamula and Brambley, 2005a] Katipamula, S. and Brambley, M. (2005a). Review Article: Methods for Fault Detection, Diagnostics, and Prognostics for

Building Systems a Review, Part I. *HVAC&R Research*, 11(2):169–187.

[Katipamula and Brambley, 2005b] Katipamula, S. and Brambley, M. (2005b). Review Article: Methods for Fault Detection, Diagnostics, and Prognostics for Building Systems a Review, Part II. *HVAC&R Research*, 11(2):169–187.

[Ma et al., 2012] Ma, Y., Kelman, A., Daly, A., and Borrelli, F. (2012). Predictive control for energy efficient buildings with thermal storage. *IEEE Control system magazine*, 32(1):44–64.

[Mulumba and Friedrich, 2014] Mulumba, T. and Friedrich, L. A. (2014). Kalman filter-based FDD for an Air Handling Unit (AHU). *15th International Refrigeration and Air Conditioning Conference at Purdue*.

[Rossi and Braun, 1997] Rossi, T. M. and Braun, J. E. (1997). A statistical, rule-based fault detection and diagnostic method for vapor compression air conditioners. *HVAC&R Research*, 3(1):19–37.

[Roth et al., 2005] Roth, K. W., Westphalen, D., Feng, M. Y., Llana, P., and Quartararo, L. (2005). Energy impact of commercial building controls and performance diagnostics: market characterization, energy impact of building faults and energy savings potential. *Prepared by TAIX LLC for the US Department of Energy. November. 412pp (Table 2–1)*.

[Schein et al., 2006] Schein, J., Bushby, S. T., Castro, N. S., and House, J. M. (2006). A rule-based fault detection method for air handling units (APAR). *Energy and Buildings*, 38(12):1485–1492.

[Usoro et al., 1985] Usoro, P., Schick, I., and Negahdaripour, S. (1985). An innovation-based methodology for hvac system fault detection. *Journal of dynamic systems, measurement, and control*, 107(4):284–289.

[Venkatasubramanian et al., 2003] Venkatasubramanian, V., Rengaswamy, R., and Kavuri, S. N. (2003). A review of process fault detection and diagnosis: Part II: Qualitative models and search strategies. *Computers & Chemical Engineering*, 27(3):313–326.

[Wang and Cui, 2005] Wang, S. and Cui, J. (2005). Sensor-fault detection, diagnosis and estimation for centrifugal chiller systems using principal-component analysis method. *Applied Energy*, 82(3):197–213.